

Structural behaviour differences in low methoxy pectin solutions in presence of divalent cations (Ca²⁺ and Zn²⁺): a process driven by the binding mechanism of the cation with the galacturonate unit

Ali Assifaoui^{1,}, Adrien Lerbret^{1,*}, Huynh T. D. Uyen¹, Fabrice Neiers², Odile Chambin¹, Camille Loupiac^{1,3}, Fabrice Cousin³*

¹ UMR PAM, AgroSup Dijon - Université de Bourgogne, Dijon, France

² CSGA, INRA-CNRS-Université de Bourgogne, Bd Sully, Dijon, France

³ Laboratoire Léon Brillouin, CEA-Saclay, Gif-sur-Yvette, France

ELECTRONIC SUPPLEMENTARY INFORMATION

Molecular dynamics simulation

We performed molecular dynamics (MD) simulations using the CHARMM program.¹ Galacturonate (Gal) was modelled with the CHARMM carbohydrate force field^{2, 3} and the TIP3P potential⁴ modified for the CHARMM force field⁵ was used to represent water. The Lennard-Jones parameters considered to represent Van der Waals interactions of Ca²⁺ and Zn²⁺ were those determined by Marchand and Roux⁶ ($\epsilon=0.12$ kcal.mol⁻¹ and $\sigma=2.44$ Å) and by Stote and Karplus⁷ ($\epsilon=0.25$ kcal.mol⁻¹ and $\sigma=1.95$ Å), respectively. The SHAKE algorithm⁸ has been used to fix the length of all covalent bonds involving an hydrogen atom as well as the geometry of water molecules. Newtonian equations of motion were integrated with the Verlet leapfrog algorithm and a time step of 1 fs. Van der Waals interactions have been force switched to zero between 10 and 12 Å and Lorentz-Berthelot mixing rules were

used for cross-interaction terms. Electrostatic interactions have been handled by the Particle Mesh Ewald (PME) method with $\kappa = 0.33 \text{ \AA}^{-1}$ and the fast-Fourier grid spacing set to $\sim 1 \text{ \AA}$.

We followed an analogous procedure as that described by Braccini and Perez^{9, 10} to build a pair of Gal chains, A and B. Each chain consisted of eight Gal units and was built in the 2_1 helical conformation, using the angles values from Scavetta *et al.*¹¹ ($\tau = \text{C1}'\text{-O4-C4} = 117^\circ$, $\phi = \text{O5}'\text{-C1}'\text{-O4-C4} = 80^\circ$, $\psi = \text{C1}'\text{-O4-C4-O5} = 161^\circ$, see Figure S1 for atom names). The two chains were superimposed in an antiparallel arrangement and aligned along the Z-axis. Then, they were rotated along the Z-axis by angles of 290° and 60° , respectively. Chain B was then translated by 6.33 \AA along the Y-axis. This distance corresponds to the one found by Braccini and Perez for the pairs of Gal chains in the egg-box configuration.¹⁰ No translation was performed along the Z-axis. To ensure the system's charge neutrality, we added four divalent ions as well as eight sodium ions in regions where their interaction with a Gal chain was the most favorable. For this purpose, we first performed grid-based energy calculations of a decameric Gal chain in vacuum with a grid size of 0.5 \AA and a dielectric constant, ϵ , of either 1, 10, 20, 40 or 80 (this allowed us to check how dependent these favorable interaction regions were on ϵ). The initial positions of zinc cations were assumed to be identical to those of calcium. This system was then put in a cubic simulation box of size $L = 47.8 \text{ \AA}$ and 3600 water molecules non overlapping with either the Gal chains or with the ions were inserted with random positions and orientations.

Initial configurations were first minimized with the steepest-descent algorithm, keeping frozen the positions of Gal chains and ions. Then, energy minimization was performed for 1000 and 2000 steps using the steepest descent and conjugate gradients algorithms, respectively, and applying harmonic constraints on the heavy atoms of Gal chains and ions. Next, the system was heated up from 100 to 300 K at a rate of 5 K/ps and equilibrated for 50 ps at 300 K in the microcanonical ensemble and then for 1 ns in the isobaric-isothermal

ensemble at a pressure of 1 atm. The average volume of the latter simulation was used in a production simulation performed in the canonical ensemble for 20 ns, the last 10 ns of which were considered for analysis.

We also performed a similar simulation of the Gal chains, where in the initial configuration the four divalent cations were substituted for Na^+ , and where four additional sodium cations were added in the simulation box to fulfill charge neutrality. In the presence of sodium, the two Gal chains dissociated quickly (data not shown). The final configuration of this simulation was then used as the initial configuration for two additional 100-ns long simulations, where we substituted four of the sodium cations for either Ca^{2+} or Zn^{2+} (we also removed four additional Na^+ for charge neutrality). These simulations aimed at investigating the ability of Ca^{2+} and Zn^{2+} to induce the association of Gal chains. We also run 50-ns long simulations of Ca^{2+} and Zn^{2+} in presence of 1000 water molecules (and 2 chloride ions for charge neutrality) to determine the average numbers of water molecules found in the first shell of these cations in the bulk.

Umbrella sampling simulations. We performed additional umbrella sampling simulations to investigate more specifically the interactions of the divalent cations with either the carboxylate group of Gal or with water. This method has already been successfully employed to investigate the interactions of divalent cations with charged residues.^{12, 13} The systems simulated to determine the potentials of mean force (PMF) for the interaction of cations with the carboxylate group of Gal consisted of a Gal monomer, a divalent cation and a chloride ion (for charge neutrality) and 500 water molecules in a cubic simulation of side length L of about 24.6 Å. The C6-cation distance, r , was considered as the reaction coordinate. Simulations of 2 ns were performed with r ranging from 2 to 8 Å, with steps Δr of 0.1 Å between 2 Å and 5 Å and of 0.25 Å between 5 Å and 8 Å (total of 43 simulations). The harmonic constant of the

restraining potential ranged from $800 \text{ kcal.mol}^{-1}.\text{\AA}^{-2}$ at short distances to $10 \text{ kcal.mol}^{-1}.\text{\AA}^{-2}$ at long ones. The Weighted Histogram Analysis Method (WHAM)¹⁴ has been employed to determine PMFs using the program of Alan Grossfield.¹⁵ The Jacobian correction¹⁶ was then added to these PMFs.

Structure of galacturonate (Gal)

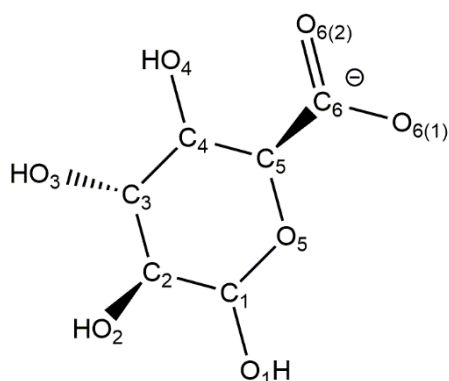


Figure S1: Schematic structure of Gal. The hydrogens bonded to the carbons from the glucose ring are not shown for clarity.

Interaction between cations and Gal

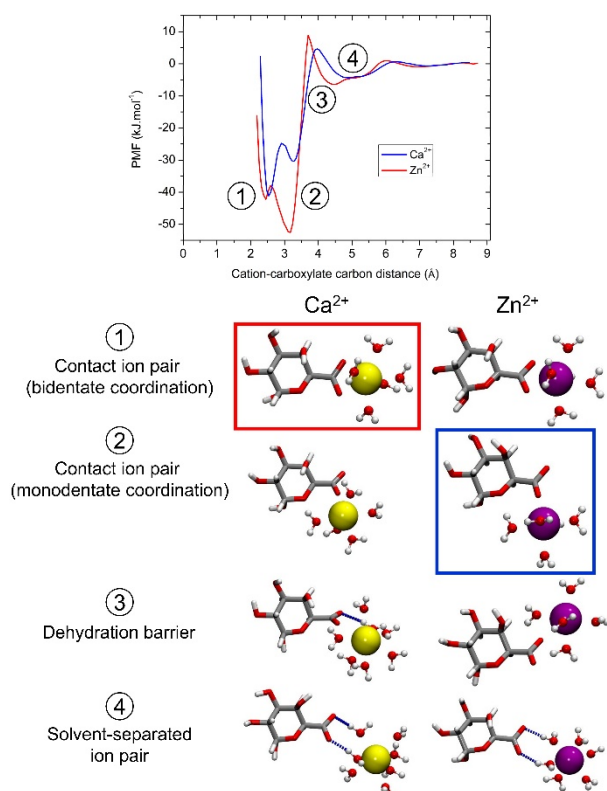


Figure S2: Potentials of mean force (PMFs) for the interaction between the divalent cations and Gal. The PMFs exhibit two deep minima, (1) and (2), where the cations are in contact with the carboxylate group of Gal in the bidentate or the monodentate coordination, respectively. The maximum (3) corresponds to the barrier for desolvating the cations, and the shallow minimum (4) indicates the solvent-separated ion pair, in which Gal and the cations share with each other their hydration water molecules. Representative configurations extracted from the umbrella sampling simulations for the two cations are displayed. For clarity, only water molecules in the first coordination shell of the cations are shown and sodium counterions are not represented. Hydrogen bonds between water and the carboxylate group of Gal are drawn as dashed blue lines. The most favorable configurations for the interaction of Ca²⁺ and Zn²⁺ with Gal are surrounded by red and blue rectangles, respectively.

Association of Gal chains

Figure S3a shows the starting configuration used to probe the ability of Ca²⁺ and Zn²⁺ to induce the association of Gal chains. In this configuration, the two Gal chains are dissociated and the divalent cations are not in contact with them. After a simulation time of 100 ns, the two chains are found associated in presence of Ca²⁺, but not in presence of Zn²⁺ (Figure S3b).

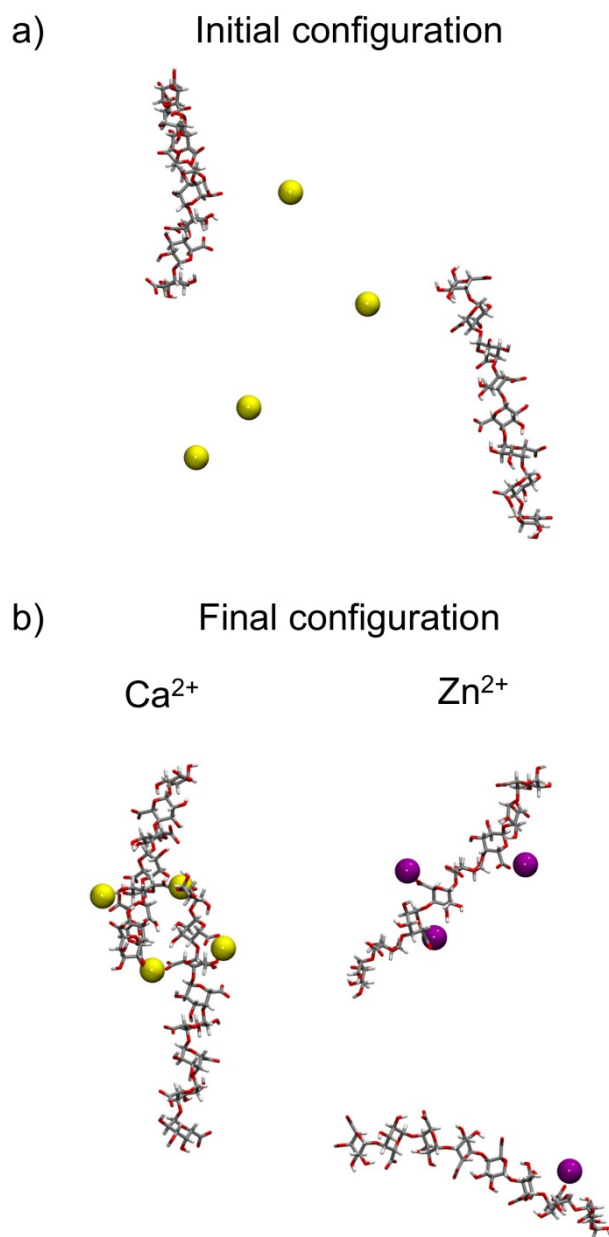


Figure S3: Configurations of two Gal chains: a) in the initial configuration ($t = 0$ ns), the two Gal chains are dissociated and none of the divalent cations is in contact with them, b) in the final configuration ($t = 100$ ns), the monocomplexation of both Ca^{2+} (left) and Zn^{2+} (right) is completed (that is, each cation is bounded to Gal), but only Ca^{2+} has induced the association of the two Gal chains via the formation of two Gal- Ca^{2+} -Gal bridges. For clarity, water molecules and sodium counterions are not shown.

Movie legends

Movie S1. Association of Gal chains in presence of Ca²⁺.

This video shows configurations extracted each ns of the 100 ns-long MD simulation of two octameric Gal chains in presence of 4 divalent calcium cations. At the end of the movie, the two chains are found associated by two Gal-Ca²⁺-Gal bridges. For clarity, water molecules and sodium counterions are not shown.

Movie S2. Association of Gal chains in presence of Zn²⁺.

This video shows configurations extracted each ns of the 100 ns-long MD simulation of two octameric Gal chains in presence of 4 divalent zinc cations. At the end of the movie, the two chains are still found dissociated, even though the monocomplexation of zinc cations is completed. For clarity, water molecules and sodium counterions are not shown.

References

1. B. R. Brooks, C. L. Brooks, A. D. Mackerell, L. Nilsson, R. J. Petrella, B. Roux, Y. Won, G. Archontis, C. Bartels, S. Boresch, A. Caflisch, L. Caves, Q. Cui, A. R. Dinner, M. Feig, S. Fischer, J. Gao, M. Hodoscek, W. Im, K. Kuczera, T. Lazaridis, J. Ma, V. Ovchinnikov, E. Paci, R. W. Pastor, C. B. Post, J. Z. Pu, M. Schaefer, B. Tidor, R. M. Venable, H. L. Woodcock, X. Wu, W. Yang, D. M. York and M. Karplus, *J. Comput. Chem.*, 2009, **30**, 1545-1614.
2. O. Guvench, S. N. Greene, G. Kamath, J. W. Brady, R. M. Venable, R. W. Pastor and A. D. Mackerell, *J. Comput. Chem.*, 2008, **29**, 2543-2564.
3. O. Guvench, E. Hatcher, R. M. Venable, R. W. Pastor and A. D. MacKerell, *Journal of Chemical Theory and Computation*, 2009, **5**, 2353-2370.
4. W. L. Jorgensen, J. Chandrasekhar, J. D. Madura, R. W. Impey and M. L. Klein, *J. Chem. Phys.*, 1983, **79**, 926-935.
5. P. Mark and L. Nilsson, *J. Phys. Chem. A*, 2001, **105**, 9954-9960.
6. S. Marchand and B. Roux, *Proteins*, 1998, **33**, 265-284.
7. R. H. Stote and M. Karplus, *Proteins*, 1995, **23**, 12-31.
8. J.-P. Ryckaert, G. Ciccotti and H. J. C. Berendsen, *J. Comput. Phys.*, 1977, **23**, 327-341.
9. I. Braccini, R. P. Grasso and S. Pérez, *Carbohydr. Res.*, 1999, **317**, 119-130.
10. I. Braccini and S. Perez, *Biomacromolecules*, 2001, **2**, 1089-1096.
11. R. D. Scavetta, S. R. Herron, A. T. Hotchkiss, N. Kita, N. T. Keen, J. A. Benen, H. C. Kester, J. Visser and F. Jurnak, *Plant Cell*, 1999, **11**, 1081-1092.
12. E. Iskrenova-Tchoukova, A. G. Kalinichev and R. J. Kirkpatrick, *Langmuir*, 2010, **26**, 15909-15919.
13. L. M. Hamm, A. F. Wallace and P. M. Dove, *J. Phys. Chem. B*, 2010, **114**, 10488-10495.
14. B. Roux, *Comput. Phys. Commun.*, 1995, **91**, 275-282.
15. A. Grossfield, "WHAM: the weighted histogram analysis method", version 2.0.6, <http://membrane.urmc.rochester.edu/content/wham>.
16. I. V. Khavrutskii, J. Dzubiella and J. A. McCammon, *J. Chem. Phys.*, 2008, **128**.